Submitted to Physical Review

UCRL-19777
Preprint

c.2

NEW DATA IN THE REACTION $\pi^+ p \to \Sigma^+ K^+$ AT 1.28 AND 1.41 GeV/c AND A TEST OF CHARGE INDEPENDENCE IN THE c.m. ENERGY RANGE 1.820 TO 2.090 GeV

G. E. Kalmus, G. Borreani, and J. Louie

July 1970

AEC Contract No. W-7405-eng-48

LAWRENCE RADIATION LABORATORY
UNIVERSITY of CALIFORNIA BERKELEY

UCRL-19777

DISCLAIMER

NEW DATA IN THE REACTION $\pi^+ p \to \Sigma^+ K^+$ AT 1.28 AND 1.41 GeV/c AND A TEST OF CHARGE INDEPENDENCE IN THE c.m. ENERGY RANGE 1.820 TO 2.090 GeV*

G. E. Kalmus, G. Borreani,† and J. Louie‡

Lawrence Radiation Laboratory
University of California
Berkeley, California 94720

July 1970

ABSTRACT

Data at two incident π^+ momenta (1.28 and 1.41 GeV/c) in the reaction $\pi^+ p \to \Sigma^+ K^+$ are presented. Our previous partial-wave analysis of this reaction[1] is extended to include these data. Charge independence is tested over the c.m. energy range 1.820 to 2.090 GeV; we used our data for the $\Sigma^+ K^+$ channel and published data for the $\pi^- p \to \Sigma^0 K^0$ and $\Sigma^- K^+$ channels.

I. INTRODUCTION

Data at two incident π^+ momenta (1.28 and 1.41 GeV/c) in the reaction $\pi^+ p \to \Sigma^+ K^+$ are presented. These data, which consist of angular distributions, Σ^+ polarizations, and cross sections, are then combined with our previously published data for seven momenta (1.34, 1.43, 1.55, 1.63, 1.68, 1.77, and 1.84 GeV/c.[1] The partial-wave analysis described in our previous paper (referred to hereafter as KBL) is extended to include these two momenta. The data are also used to make a test of charge independence in Σ production. We used published data for the channels $\pi^- p \to \Sigma^0 K^0$ and $\pi^- p \to \Sigma^- K^+$ in the same energy range. Since nearly all the experimental details, theory, and analyses are identical to those in KBL, only a brief description of the essentials is given in each of these sections, and the reader is referred to KBL for a full discussion. The tables and figures have, wherever appropriate, included our previous data; however, for angular distributions, polarizations, Argand plots, and tables of the parameters of the fits, the reader is again referred to KBL.

II. EXPERIMENTAL DETAILS

A. Exposure

The experiment consisted of an exposure of the Lawrence Radiation Laboratory 25-inch hydrogen bubble chamber to a π^+ beam of momenta 1.28 and 1.41 GeV/c. Approximately 130 000 pictures were taken at each momentum. Table I summarizes the data taken.

B. Scanning and Measuring

The entire film was scanned and half of it (every other roll) was rescanned for "two-prong" events in which one or both prongs were "kinked." The scanning efficiency of each scan was found to be about 90% for events that were eventually accepted as $\pi^+ p \to \Sigma^+ K^+$. All events that were found on either scan were measured by use of the COBWEB on-line Franckenstein system.[2] Events were remeasured if they did not fit, with a satisfactory χ^2, the hypothesis $\pi^+ p \to \Sigma^+ K^+$, with the Σ^+ decaying either to $\pi^+ n$ or $p\pi^0$. The second measurement yielded approximately an additional 20% of events. The events that still failed were examined on the scan table. Approximately another 5% appeared to have a good Σ^+, and were within the cuts made on the data. However, in most cases the reason for failure was clear (such as a confused vertex) and independent of the kinematics. [At 1.28 GeV/c the energy is below threshold for additional π^0 production, whereas at 1.41 GeV/c

all events were also fitted to the hypotheses $\Sigma^+K^+\pi^0$ and $\Sigma^+\pi^+K^0$. However, only four events (out of about 300) fitted either of these.] These failures were therefore essentially unbiased, and were corrected for only in the cross-section measurement.

Cuts were made on the data for beam entry angle and momentum, for fiducial volume, Σ^+ length (> 0.3 cm), and $\Sigma^+ \to \pi^+ n$ decay angle (> 5°). The remaining events were then weighted to take these cuts into account (for details, see KBL).

In order to obtain cross sections, beam tracks were counted every hundredth frame throughout the entire film.

III. DATA

A. Cross Sections

Table II shows the number of events obtained at each momentum, and the calculated cross sections. Figure 1 shows the cross sections together with others in the same energy range from the literature. The cross sections were obtained by using only the weighted number of $\Sigma^+ \to \pi^+ n$ events (and multiplying by 2.12 to take into account the $\Sigma^+ \to p\pi^0$ decay mode).[7] The errors shown include both statistical and systematic effects.

B. Angular Distributions

The angular distributions for both the weighted and unweighted $\pi^+ p \to \Sigma^+ K^+$, $\Sigma^+ \to \pi^+ n$ events are shown in Fig. 2. The production cosine, $\cos\theta$, is defined as the cosine of the angle in the center-of-mass system between the incident π^+ and outgoing K^+.

C. Polarizations

Fig. 3 shows $\alpha \overline{P}_\Sigma$ (for $\Sigma^+ \to p\pi^0$) as a function of $\cos\theta$, where α is the Σ^+ decay asymmetry parameter and $\overline{P}_\Sigma$ is the average polarization of the Σ. (See KBL for more details.)

D. Legendre Expansions

Figure 4 shows the values of A_m/A_0 of the Legendre polynomials fitted to the experimental distributions shown in Fig. 2. The expression

$$dN/d(\cos\theta) = \sum_{m=0}^{mmax} A_m P_m(\cos\theta)$$

was used. Figure 5 shows the values of the expansion coefficients B_n/A_0 of the first associated Legendre series when fitted to the polarization distributions shown in Fig. 3. An expression of the form

$$I\underline{P} = \hat{n} \sum_{n=1}^{nmax} B_n P_n^1(\cos\theta)$$

was used, where I is the angular distribution, $\underline{P}$ the polarization, and $\hat{n}$ a unit vector along the production normal [$\hat{n} = (\hat{\pi}^+ \times \hat{K}^+)/(|\hat{\pi}^+ \times \hat{K}^+|)$, $\hat{\pi}^+$ and $\hat{K}^+$ are unit vectors along the π^+ and K^+ directions].

The A_m/A_0 values plotted come from the seventh-order fit. It was found that a third-order fit was satisfactory at 1.28 GeV/c and a fourth-order fit at 1.41 GeV/c. (A_1/A_0 to A_4/A_0 remained essentially unchanged between the fourth- and seventh-order fits.) The B_n/A_0 values plotted come from a fourth-order fit (the maximum allowed with five data points). It was found that a second-order fit was satisfactory at 1.28 and a third-order at 1.41 GeV/c.

IV. THEORY

Partial-Wave Analysis

Since the theory for the partial-wave analysis is identical to that used in our previous paper,[1] only a very brief outline is given here.

In the reaction of spin 0 + spin 1/2 → spin 0 + spin 1/2 the transition operator M is given by $M = a(\theta) + b(\theta)\, \underline{\sigma}\cdot\hat{n}$, where a and b are the non-spin-flip and spin-flip amplitudes, respectively. The production angle θ and production normal $\hat{n}$ have been defined in Sec. IIIB, D, and $\underline{\sigma}$ is the Pauli spin operator.

The relationships between $a(\theta)$ and $b(\theta)$ and the complex partial-wave amplitudes $T_\ell^\pm$ (ℓ is the final orbital angular momentum) are

$$a(\theta) = \lambda\Sigma_{\ell}[(\ell + 1)T_{\ell}^{+} + T_{\ell}^{-}]\ P_{\ell}(\cos\theta),$$

$$b(\theta) = i\lambda\Sigma_{\ell}[T_{\ell}^{+} - T_{\ell}^{-}]\ P_{\ell}^{1}(\cos\theta),$$

where λ is the π^+ wavelength in the c.m. system divided by 2π, the superscripts $\pm$ refer to $J = \ell \pm 1/2$, and P_ℓ and P_ℓ^1 are the ℓth-order Legendre and first associated Legendre polynomials respectively.

The differential cross section I and polarization $\underset{\sim}{P}$ are given by

$$I\left(=\frac{d\sigma}{d\Omega}\right) = |a|^2 + |b|^2$$

and

$$I\underset{\sim}{P} = 2\ \mathrm{Re}(a^{*}b)\hat{n}.$$

The amplitudes $T^{\pm}$ are in general functions of the c.m. energy.

In our analysis we have assumed that the energy dependence of T was given by the Breit-Wigner formula for a resonance

$$T = \left\{1/2(\Gamma_e\Gamma_r)^{1/2}/[(E_R - E) - i\Gamma/2]\right\} e^{i\phi},$$

where E is the c.m. energy, E_R is the energy of the resonance, Γ_e the partial width into the elastic and Γ_r the partial width into the final (reaction) channel, and Γ the total width $= \Sigma_i \Gamma_i$, where i are all the decay channels. We have also assumed that the partial widths Γ_i are energy dependent and that these can be approximated by the Glashow-Rosenfeld formula[8]

$$\Gamma_i \propto \left[\frac{q_i^2}{q_i^2 + X^2}\right]^{\ell_i} \frac{q_i}{E},$$

where q_i and ℓ_i are the momentum and orbital angular momentum of the decay products of the resonance into the ith channel, and X is a parameter associated with the radius of the interaction and has the dimensions of mass (we use X = 350 MeV).

The form of the energy dependence used for the nonresonant amplitudes was

$$T = (A + Bk)e^{i(C + Dk)},$$

where k is the incident c.m. momentum.

Values for $(\Gamma_e\Gamma_r)$, E_R, $\Gamma/2$, and ϕ or A, B, C, and D (or both) were obtained for each partial wave by minimizing the χ^2 between the experimental angular distributions, polarizations, and cross sections and those calculated for various values of the input parameters (see KBL).

V. RESULTS

A. s-Channel Partial-Wave Analysis

Since the two momenta are on the low side of our previous range, and on the low side of the $\Delta^{++}(1950)$, we decided to concentrate only on the s-channel partial-wave analysis rather than the s-, t-, and u-channel approach also used in KBL. As these data show only a small increase, both in statistics and in energy range, over our previous data, we have used our previous solutions[1] (based on seven momenta) as starting values for all nine momenta. Clearly, any solution that did not fit the data well before would still not fit. Some of the parameters of the fits are given in Table III. The fit numbers are the same as in KBL, and indicate that the final solution in KBL was used as the initial condition here. It can be seen from this that the solutions are little changed. Figures 6a and b show two Argand plots, for solutions 192B and 209B. In particular, the amplitude of the $\Delta(1950)$ is within errors of the previous value [and thus the branching fraction for $\Delta(1950) \to \Sigma^+K^+$ of $2.0 \pm 0.4\%$ remains unchanged]. The only difference appears to be in the width of the $\Delta(1950)$, which has increased slightly, but is still within the error limits quoted in KBL. Thus, all conclusions reached in our previous paper remain valid.

VI. TEST OF CHARGE INDEPENDENCE IN Σ PRODUCTION

A. Introduction

Charge independence in strong interactions

predicts definite relationships between the amplitudes of the reactions

$$\pi^+ p \to \Sigma^+ K^+, \quad (1)$$

$$\pi^- p \to \Sigma^0 K^0 \quad (2)$$

and

$$\pi^- p \to \Sigma^- K^+ . \quad (3)$$

If the amplitudes of these reactions are $f^+(\theta)$, $f^0(\theta)$, and $f^-(\theta)$, respectively, then for each spin state the following relationship holds:

$$f^+(\theta) = 2f^0(\theta) + f^-(\theta) . \quad (4)$$

This corresponds to a triangle in the complex plane.

Since the differential cross sections are the squares of the amplitudes, the following "triangle inequalities" between the cross sections (for each spin state) hold:

$$\left(2\frac{d\sigma}{d\Omega}\bigg|_{\Sigma^0}\right)^{1/2} \leqslant \left(\frac{d\sigma}{d\Omega}\bigg|_{\Sigma^+}\right)^{1/2} + \left(\frac{d\sigma}{d\Omega}\bigg|_{\Sigma^-}\right)^{1/2}, \quad (5)$$

$$\left(\frac{d\sigma}{d\Omega}\bigg|_{\Sigma^+}\right)^{1/2} \leqslant \left(2\frac{d\sigma}{d\Omega}\bigg|_{\Sigma^0}\right)^{1/2} + \left(\frac{d\sigma}{d\Omega}\bigg|_{\Sigma^-}\right)^{1/2}, \quad (6)$$

$$\left(\frac{d\sigma}{d\Omega}\bigg|_{\Sigma^-}\right)^{1/2} \leqslant \left(2\frac{d\sigma}{d\Omega}\bigg|_{\Sigma^0}\right)^{1/2} + \left(\frac{d\sigma}{d\Omega}\bigg|_{\Sigma^+}\right)^{1/2} . \quad (7)$$

In fact, it can be shown that the relationships (5)-(7) also hold after summing over spins.

The purpose of this section of the paper is to test these inequalities, using our data (including KBL) and published data at 1.277, 1.325, 1.50, 1.60, 1.70, and 1.86 GeV/c in the reactions $\pi^- p \to \Sigma^0 K^0$ and $\pi^- p \to \Sigma^- K^+$.[9-11]

A test of this kind has been performed by Binford et al.[12] at three lower momenta (up to 1.277 GeV/c) and by Pan and Forman[5] at 1.7 GeV/c. Binford et al. find that relationship (5) becomes an equality as $\cos\theta \to +1$ (in fact, it is slightly violated), whereas Pan and Forman find that relationship (6) is violated near $\cos\theta = -1$.

B. Method

For the purpose of this paper we have used the fitted A_n coefficients [where $d\sigma/d\Omega = \sum_n A_n P_n(\cos\theta)$ has been used] to represent the data. Table IV gives the A_n coefficients at our nine momenta for $\pi^+ p \to \Sigma^+ K^+$. We have also interpolated between our data points to obtain values of A_n for 1.5, 1.6, and 1.7 GeV/c in order to perform the tests at momenta for which data in the other channels are available. The A_n coefficients for $\pi^- p \to \Sigma^0 K^0$ and $\pi^- p \to \Sigma^- K^+$ were taken from Refs. 9 — 11.

C. Results

We have plotted only two of the inequalities at each momentum (expressions 5 and 6), since for expression (7) the left hand side (lhs) was found to be consistently less than the right hand side (rhs).

Figures 7a–f show the tests of the triangle inequalities at 1.28, 1.43, 1.50, 1.60, 1.70, and 1.76 GeV/c. The broken lines represent the (rhs) of expression (6) for the upper figure (I) and the rhs of (5) for the lower figure (II). The dotted lines represent the lhs of (6) for (I) and the lhs of (5) for (II). Thus (5) and (6) are satisfied if the dotted line remains below the broken line. In order to clarify the drawings, in the cases where there is no "violation" at any angle, we have not indicated the errors. Where there is a crossing of the curves we have drawn two regions--corresponding to ± 1 standard deviation for the lhs and rhs of (6) or (5). Charge independence, therefore, requires that the lower dotted line not be significantly higher than the upper broken line.

By examining Fig. 7 we note the following:

(a) There is no clear evidence for a violation of charge independence although at the upper four momenta the mean value of the lhs of (6) is greater than the mean value of the rhs in the forward direction. At the two momenta closest to the $\Delta^{++}(1950)$ the extent of this effect is greatest, extending from $\cos\theta = 0.75$ to 1.0 at 1.5 GeV/c and from $\cos\theta = 0.1$ to 1.0 at 1.6 GeV/c.

(b) As the momentum increases the triangle

(Fig. 8) becomes flatter, and relation (6) becomes an equality (i. e. $\phi \to 0$ deg)--first in the forward direction at 1.5 GeV/c and then extending over the whole range in cos θ.

(c) At the lowest momentum (1.28 GeV/c), relation (5) becomes an equality in the forward direction (i. e., $\phi' \to 180$ deg). The general behavior (that ϕ' increases as cos θ increases) persists at all momenta.

D. Discussion

1. Our results are perfectly consistent with those of Binford et al.[12] at the lowest momentum and with Pan and Forman[5] at 1.7 GeV/c. This is not surprising, since in each case the same $\pi^- p \to \Sigma^0 K^0$ and $\Sigma^- K^+$ data were used and the only difference was in the $\Sigma^+ K^+$ data.

2. Since there appears to be a persistent, but statistically not very significant, violation of condition (6), we have examined the data in the region close to cos $\theta = 1.0$ carefully and, in particular, the data of Dahl et al.,[11] which were used at 1.5 GeV/c and above for both $\Sigma^0 K^0$ and $\Sigma^- K^+$. It was found that at 1.5, 1.7, and 1.86 GeV/c the actual angular distribution was considerably higher than the fit obtained by Dahl et al. using the Legendre polynomials, in the forward bin ($0.9 < \cos\theta < 1.0$) for the $\Sigma^0 K^0$ channel. This amounted to 1.2 σ at 1.5 GeV/c, 2σ at 1.6 GeV/c, and about 3 σ at 1.86 GeV/c, where σ is the standard deviation of the Legendre fit in that bin (not the standard deviation on the data points). This effect can be seen qualitatively in Fig. 2 in the paper by Dahl et al.[11] In addition, in the $\Sigma^- K^+$ channel the data in the same bin are also clearly higher than the curve for the fit at 1.5 and 1.7 GeV/c. The effect of this is to increase the value of the rhs of condition (6) in the region above cos $\theta = 0.9$, and therefore tends to reduce any violation of condition (6).

It should be noted that at 1.6 and 1.7 GeV/c the angular distribution of $\Sigma^0 K^0$ is forward peaked with no events in the backward direction, whereas the angular distribution of $\Sigma^- K^+$ is backward peaked with no events in the forward direction. Therefore, assuming no violation of charge independence, the triangle has to be flat with $(d\sigma/d\Omega_{|\Sigma^+}) = (2d\sigma/d\Omega_{|\Sigma^0})$ in the forward direction and $(d\sigma/d\Omega_{|\Sigma^+}) = (d\sigma/d\Omega_{|\Sigma^-})$ in the backward direction. In both these directions the two isospin amplitudes have to be relatively real. In the backward direction they are in phase, whereas in the forward direction they are 180 deg out of phase.

The relative realness of these amplitudes would result if the reactions proceeded via a particle-exchange mechanism. Thus K^* exchange in the forward direction and Λ exchange in the backward direction could be used as an explanation for the flatness of the triangle. However, at energies close to or below the $\Delta(1950)$ this interpretation is clearly not valid. Binford et al.[12] have also pointed out this curious behavior.

Finally, a higher-precision test of the triangle inequalities at about 1.6 GeV/c would be extremely interesting.

ACKNOWLEDGMENTS

We thank Glenn Eckman and the 25-inch Bubble Chamber crew and the Bevatron Operations staff for their efforts during the exposure. In addition, we thank the scanners and measurers of the Powell-Birge group for their efforts during the data-reduction phase of the experiment. Finally, we are indebted to Jane Kennedy for her help in assembling and organizing material for the paper.

FOOTNOTES AND REFERENCES

*Work done under auspices of the U. S. Atomic Energy Commission.

†Present address: Istituto di Fisica dell' Universita, Torino, Italy.

‡Present address: Brookhaven National Laboratory, Upton, Long Island, New York.

1. G. E. Kalmus, G. Borreani, and J. Louie (Lawrence Radiation Laboratory Report UCRL-19735, March 1970), submitted to Phys. Rev.
2. H. C. Albrecht, E. P. Binnall, R. W. Birge, M. H. Myers, and P. W. Weber, Lawrence Radiation Laboratory Report UCRL-18528 Rev., Oct. 1968 (unpublished).
3. C. Baltay, H. Courant, W. J. Fickinger, E. C. Fowler, H. L. Kraybill, J. Sandweiss, J. R. Sanford, D. L. Stonehill, and H. Taft, Rev. Mod. Phys. 33, 374 (1961).
4. H. W. J. Foelsche, A. Lopez-Cepero, C. Y. Chien, and H. L. Kraybill, submitted to XIIth International Conference on High Energy Physics, Dubna, 1964 (unpublished).
5. Y. L. Pan and F. L. Forman, Nucl. Phys. B16, 61 (1970).
6. P. Daronian, A. Daudin, M. A. Jabiol, C. Lewin, C. Kochowski, B. Ghidini, S. Montelli, and V. Picciarelli, Nuovo Cimento 41, 771 (1966).
7. We have used the value of the $\Sigma^+ \to \pi^+ n$ branching fraction given in the Review of Particle Properties, Rev. Mod. Phys. 41, 109 (1969), to be consistent with Ref. 1.
8. S. L. Glashow and A. H. Rosenfeld, Phys. Rev. Letters 10, 192 (1963).
9. M. L. Good and R. R. Kofler, Phys. Rev. 183, 1142 (1969).
10. T. O. Binford, M. L. Good, V. G. Lind, D. Stern, R. Krauss, and E. Dettman, Phys. Rev. 183, 1134 (1969).
11. O. I. Dahl, L. M. Hardy, R. I. Hess, T. Kirz, D. H. Miller, and T. A. Schwartz, Phys. Rev. 163, 1430 (1967), and errata, Phys. Rev. 183, 1520 (1969).
12. T. O. Binford, M. L. Good, and R. R. Kofler, Phys. Rev. 183, 1148 (1969).

Table I. Summary of film used in this experiment.

π^+ Momentum (GeV/c)	Number of pictures (1000)	Chamber used (in.)	Cross section for one event (μb) (approx)
1.28[a]	127	25	0.6
1.34	52	72	0.4
1.41[a]	130	25	0.6
1.43	41	72	0.5
1.55	121	25	0.8
1.63	164	25	0.5
1.68	47	72	0.5
1.77	122	25	0.7
1.84	119	25	0.9

a. This experiment.
Other momenta from Ref. 1

Table II. Summary of data and cross sections for $\pi^+ p \to \Sigma^+ K^+$.

Momentum of π^+ (GeV/c)	Energy c.m. (GeV/c)	Number of events			Cross section $\pi^+ p \to \Sigma^+ K^+$ (μb)
		$\Sigma^+ \to p\pi^0$ (unwtd)	$\Sigma^+ \to \pi^+ n$ (unwtd)	$\Sigma^+ \to \pi^+ n$ (wtd)	
1.28[a]	1.821	118	165	208	340 ± 35
1.34	1.851	249	290	367	400 ± 35
1.41[a]	1.886	150	238	301	490 ± 45
1.43	1.896	222	293	374	510 ± 40
1.55	1.955	142	219	279	530 ± 50
1.63	1.992	255	299	375	470 ± 40
1.68	2.016	197	299	377	505 ± 40
1.77	2.057	129	209	265	415 ± 50
1.84	2.089	102	158	201	405 ± 50

a. This experiment.
Other momenta are from Ref. 1.

Table III. Characteristics of various fits to the data.

	Fit number							
	217B	192B	194B	211B	219B	218B	215B	209B
S1	B	B	B	B	B	B	B	B*
P1	B	B	B	B	B	B	B	B
P3	B	B	B	B	B	R	B	B
D3	B	B	B	B	R	B	B	B
D5	B	B	B	R	B	B	R	B
F5	B	B	R	B	B	B	R	B
F7	B	R	R	R	R	R	R	R
G7	-	-	-	-	-	-	-	-
Degrees of freedom	137	138	138	138	138	138	138	139
χ^2	175	162	167	158	155	164	157	160
Confidence level	0.015	0.081	0.045	0.12	0.15	0.066	0.13	0.10
Resonance parameters								
Partial wave							D5	
Amplitude							0.05	
Mass (MeV)							1917	
Width (MeV)							38	
Partial wave			F5	D5	D3	P3	F5	
Amplitude			0.03	0.05	0.03	0.11	0.03	
Mass (MeV)			2055	1918	1896	2499	2055	
Width (MeV)			144	38	42	2463	114	
Partial wave		F7	F7	F7	F7	F7	F7	F7
Amplitude		0.092	0.083	0.089	0.091	0.085	0.088	0.091
Mass (MeV)		1918	1918	1970	1967	1924	1975	1973
Width (MeV)		360	314	364	318	500	366	278
Comments			a	b	c	d	b	e

B denotes a background partial wave of the form $(A + Bk)e^{i(C + Dk)}$; B* denotes a background partial wave of the form $(A + Bk)e^{iC}$. R denotes a resonant partial wave. Amplitude is defined as $(\Gamma_e\Gamma_r)^{1/2}$. Width is full width (Γ).

a. F5 amplitude small.

b. Width of D5 small compared with energy separation of data points.

c. Width of D3 small compared with energy separation of data points.

d. Mass of P3 outside energy range of data.

e. Energy dependence of phase of S1 held at zero.

Table IV. Legendre polynomial coefficients.

	P_{π^+}								
	1.28	1.34	1.41	1.43	1.55	1.63	1.68	1.77	1.84
A_1/A_0	-0.46 (±0.14)	-0.18) (±0.10)	-0.26 (±0.12)	-0.05 (±0.12)	0.15 (±0.13)	-0.19 (±0.11)	-0.02 (±0.11)	0.16 (±0.21)	0.22 (±0.17)
A_2/A_0	0.02 (±0.19)	0.05 (±0.15)	0.31 (±0.17)	0.56 (±0.16)	0.38 (±0.18)	0.60 (±0.15)	0.57 (±0.16)	0.86 (±0.21)	0.96 (±0.24)
A_3/A_0	1.12 (±0.24)	1.13 (±0.20)	0.93 (±0.22)	1.38 (±0.20)	1.42 (±0.23)	0.66 (±0.19)	0.88 (±0.20)	0.38 (±0.25)	0.65 (±0.29)
A_4/A_0	0.13 (±0.37)	0.41 (±0.23)	0.42 (±0.27)	0.49 (±0.24)	0.81 (±0.25)	0.42 (±0.21)	0.92 (±0.21)	1.26 (±0.27)	1.13 (±0.32)
A_5/A_0	0.38 (±0.41)	0.26 (±0.34)	0.22 (±0.33)	0.57 (±0.32)	0.29 (±0.27)	0.19 (±0.25)	0.45 (±0.23)	0.36 (±0.30)	0.84 (±0.36)
A_6/A_0	-0.13 (±0.44)	0.51 (±0.35)	0.33 (±0.34)	0.40 (±0.30)	1.02 (±0.30)	0.80 (±0.26)	1.12 (±0.25)	0.72 (±0.32)	1.26 (±0.37)
A_7/A_0	-0.57 (±0.77)	0.37 (±0.41)	0.37 (±0.46)	-0.24 (±0.40)	-0.22 (±0.38)	-0.07 (±0.27)	0.12 (±0.28)	0.11 (±0.38)	0.37 (±0.38)

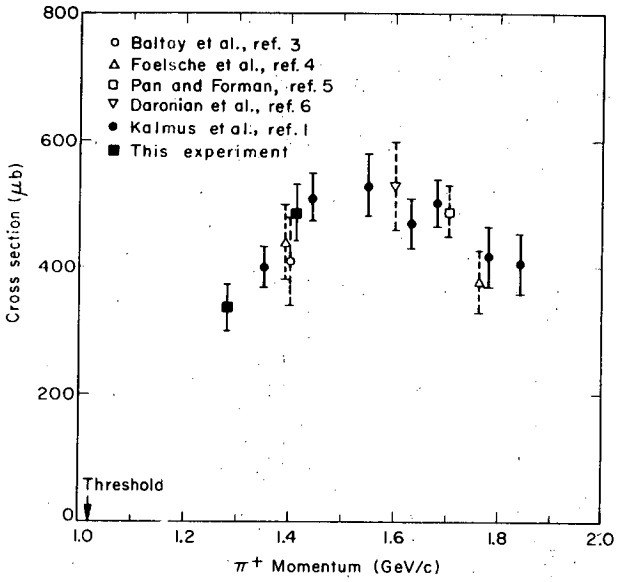

Fig. 1. $\pi^+ p \rightarrow \Sigma^+ K^+$ cross sections together with others from the literature.
XBL 703-2618

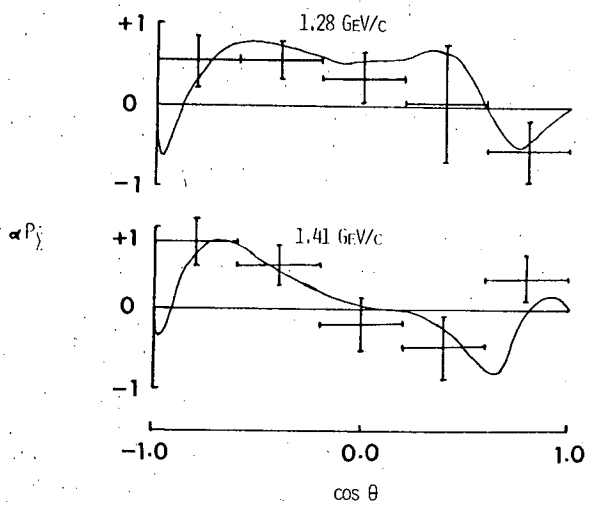

Fig. 3. $\alpha \overline{P}_\Sigma$ (for $\Sigma^+ \rightarrow p\pi^0$) as a function of cos θ at 1.28 and 1.41 GeV/c. The curves are from Fit 192B (not the fit to the first associated Legendre series).
XBL 707-1580

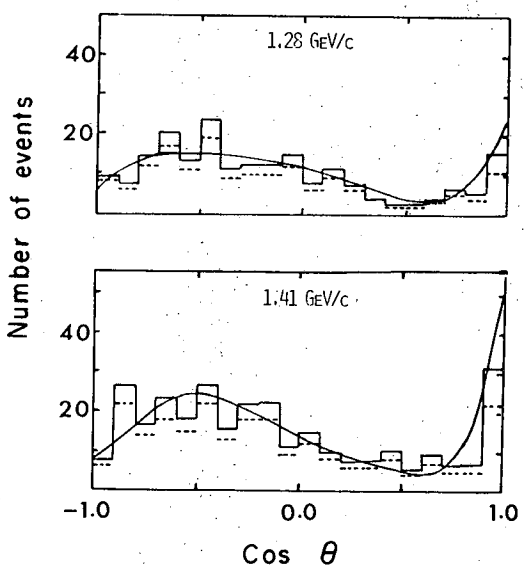

Fig. 2. Production angular distribution of $\pi^- p \rightarrow \Sigma^+ K^+$ (with $\Sigma^+ \rightarrow \pi^+ n$) at 1.28 and 1.41 GeV/c. Cos θ is defined as the cosine of the angle in the c.m. between the incident π^+ and the outgoing K^+. The curves are from Fig. 192B (not the fit to the Legendre series).
XBL 707-1579

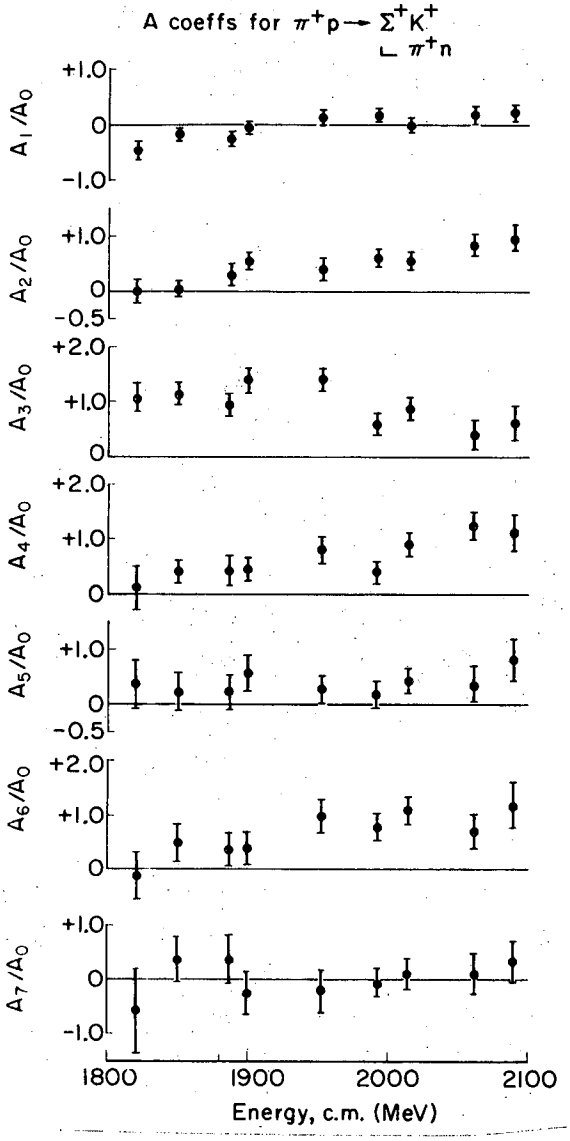

Fig. 4. Values of the Legendre polynomial coefficients A_m/A_0 from this experiment and from Ref. 1, as a function of c. m. energy. XBL703-2620

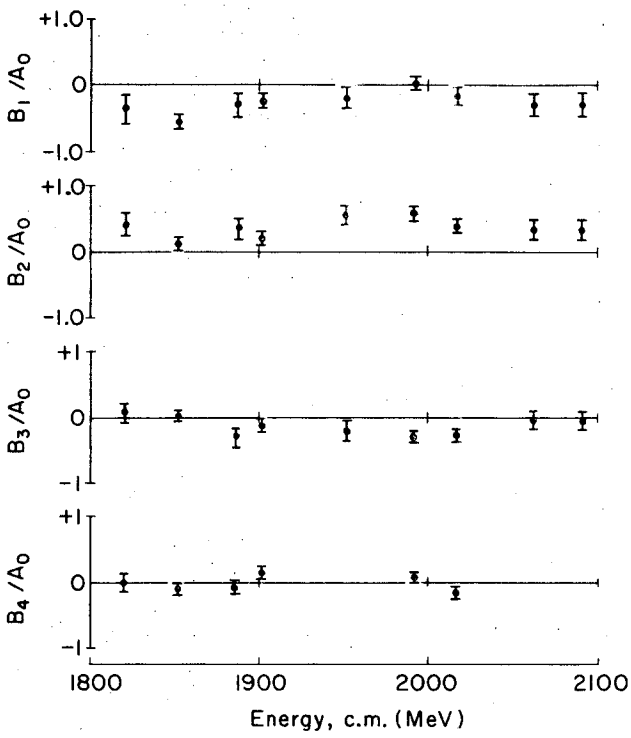

Fig. 5. Values of the first associated Legendre polynomial coefficients B_n/A_0 from this experiment and from Ref. 1 as a function of c. m. energy. XBL703-2622

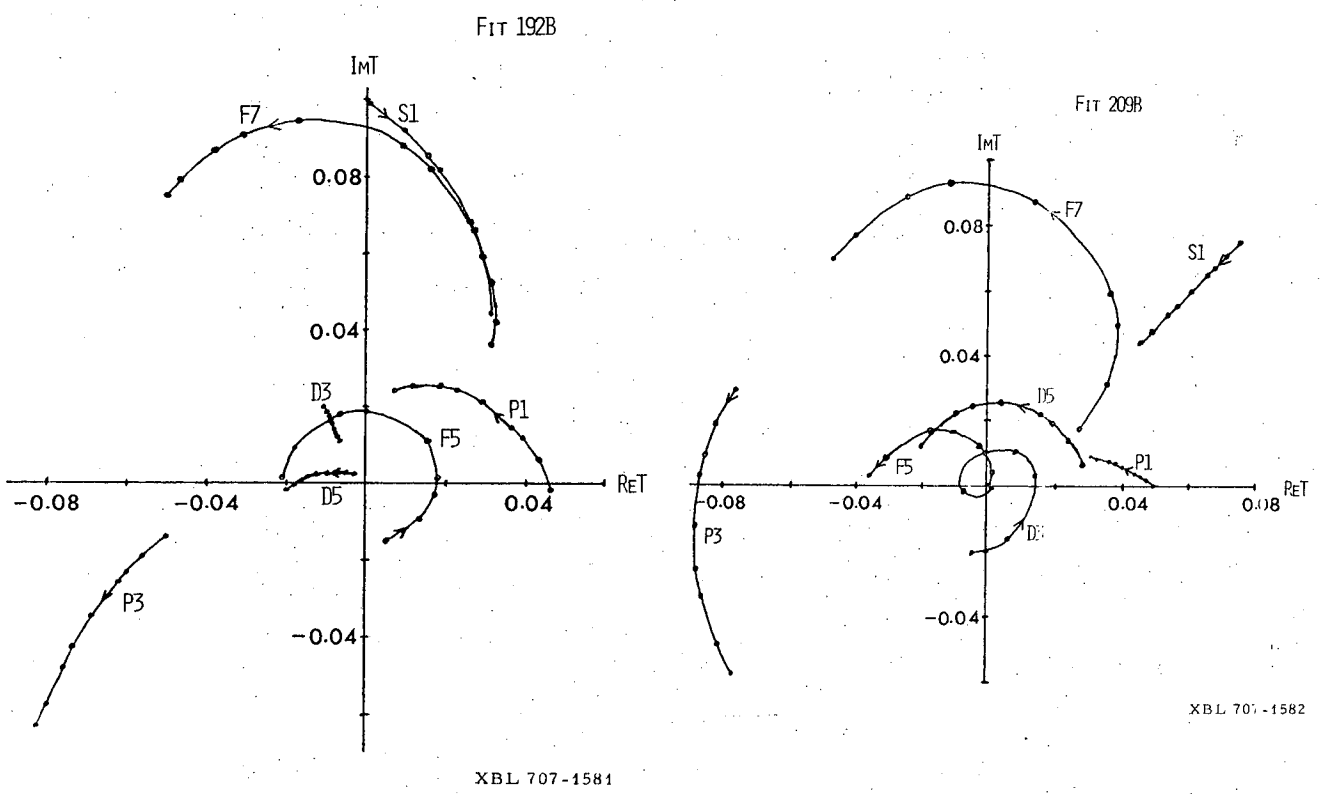

Fig. 6. Argand plots for Fits 192B and 209B. For the parameters of these fits see Table III.

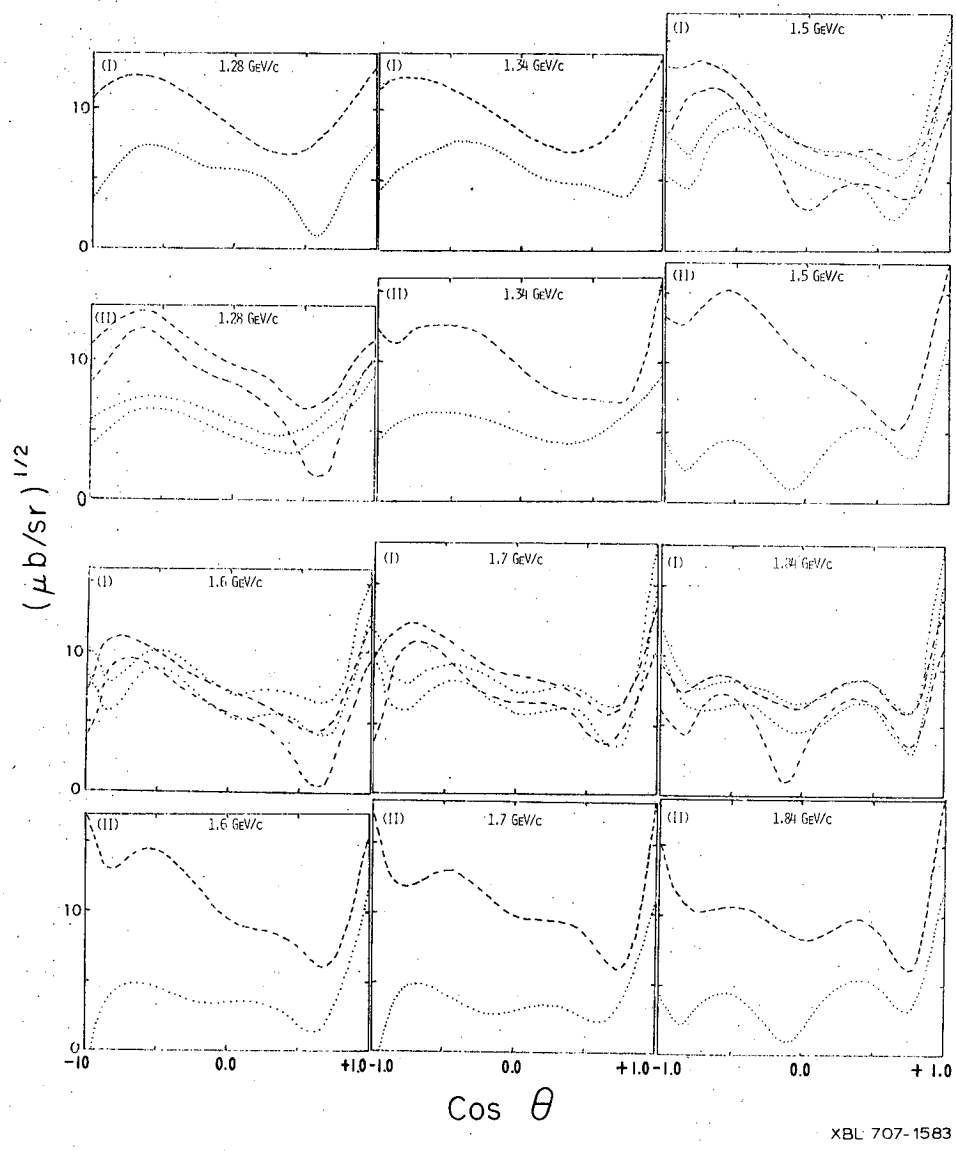

Fig. 7. I. Test of triangle inequality (6).

Broken line: $\left(2\frac{d\sigma}{d\Omega}\Big|_{\Sigma^0}\right)^{1/2}+\left(\frac{d\sigma}{d\Omega}\Big|_{\Sigma^-}\right)^{1/2}$; dotted line: $\left(\frac{d\sigma}{d\Omega}\Big|_{\Sigma^+}\right)^{1/2}$.

II. Test of triangle inequality (5).

Broken line: $\left(\frac{d\sigma}{d\Omega}\Big|_{\Sigma^-}\right)^{1/2}+\left(\frac{d\sigma}{d\Omega}\Big|_{\Sigma^+}\right)^{1/2}$; dotted line: $\left(2\frac{d\sigma}{d\Omega}\Big|_{\Sigma^0}\right)^{1/2}$.

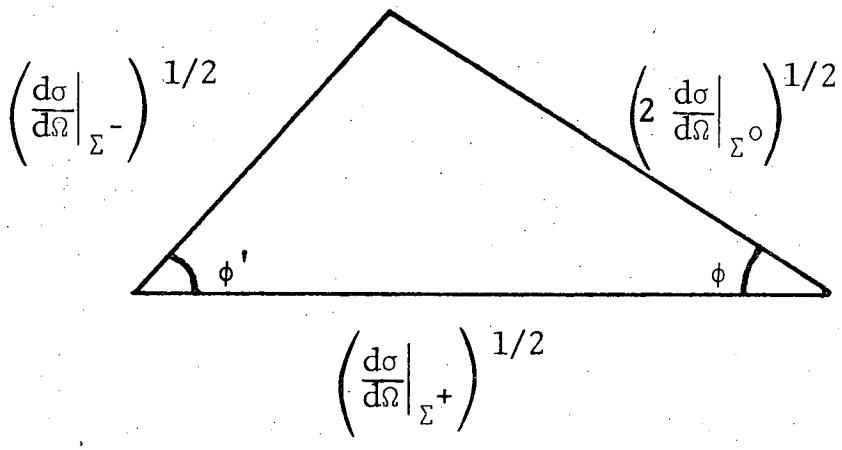

Fig. 8. Charge independence requires that the appropriate square roots of the cross sections form a closed triangle. This is illustrated here.

LEGAL NOTICE

TECHNICAL INFORMATION DIVISION
LAWRENCE RADIATION LABORATORY
UNIVERSITY OF CALIFORNIA
BERKELEY, CALIFORNIA 94720